UNIVERSITY OF CALIFORNIA SAN DIEGO

Conditional depletion of ALG-1 and ALG-2 using auxin inducible degron 2 (AID2)

A thesis submitted in partial satisfaction of the
requirements for the degree
Master of Science

in

Biology

by

Runtian Jiang

Committee in charge:

Professor Amy Pasquinelli, Chair
Professor Jens Lykke-Andersen
Professor Emily Troemel

2022

The thesis of Runtian Jiang is approved, and it is acceptable in quality and form for publication on microfilm and electronically.

University of California San Diego

2022

TABLE OF CONTENTS

LIST OF FIGURES

ABSTRACT OF THE THESIS

Conditional depletion of ALG-1 and ALG-2 using auxin inducible degron 2 (AID2)

by

Runtian Jiang

Master of Science in Biology

University of California San Diego, 2022

Professor Amy Pasquinelli, Chair

MicroRNAs (miRNAs) are small (~22 nucleotides) non-coding RNAs that target and repress messenger RNAs through imperfect base-pairing. First discovered in the nematode *Caenorhabditis Elegans* (*C. elegans*) (Lee et al., 1993), the microRNA pathway is conserved in many species ranging from humans to plants and plays important roles regulating genes that are critical for proper development, stress responses, and aging. (Bartel, 2018).

An essential component of the microRNA pathway is the Argonaute protein. In *Caenorhabditis elegans (C. elegans)*, the microRNA pathway involves two major Argonautes: Argonaute-like Gene 1 (ALG-1) and ALG-2. By knocking down ALG-1 and ALG-2 at different timepoints, one could shut down the entire microRNA pathway to study its effects under different biological contexts. I created and verified *C. elegans* strains that can rapidly degrade ALG-1 and/or ALG-2 using the auxin inducible degron 2 (AID2) system,

which is detailed in chapter 2.

Additionally, I tested if *alg-1* mRNA might be regulated by the microRNA pathway based on noncanonical microRNA binding sites located within its 5'UTR. I found that removal of the two let-7 binding sites identified in the *alg-1* 5'UTR does not result in altered expression of ALG-1, which is detailed in chapter 3.

Chapter 1

Introduction

MicroRNA Biogenesis and Targeting

During miRNA biogenesis, miRNA genes are initially transcribed as primary microRNAs (pri-miRNAs) then cleaved by the protein complex microprocessor into precursor miRNAs (pre-miRNA) that carry the mature microRNA sequence in the stems of a short hairpin loop (Denli et al., 2004). After the double-stranded pre-miRNAs leaves the nucleus, it will be processed by the protein Dicer into two ~22 nucleotide single-stranded RNA products (Grishok et al., 2001). One of the single-stranded RNAs will be loaded into the protein Argonaute (AGO), becoming the mature miRNA, and assemble into a miRNA-induced silencing complex (miRISC) (Filipowicz, 2005). The miRISC binds to a target mRNA through imperfect base-pairing between the mRNA and miRNA, then recruits proteins, which ultimately facilitate target mRNA degradation or translational inhibition (Bartel, 2018). miRISC targeting specificity is achieved by miRNA sequence complementary to its mRNA target. Specifically, nucleotides 2-8 at the 5' end of miRNA called the seed sequence can recognize complementary seed sites, which are most typically embedded within the 3’UTR of target mRNAs (Bartel, 2009). MicroRNAs can share the same seed sequence and thus are classified as members of microRNA families, whereas singletons have unique seed sequences and target specificity. (Lewis et al., 2003; Alvarez-Saavedra & Horvitz, 2010)

C. elegans miRNA Argonaute Proteins ALG-1 and ALG-2

There are 26 Argonaute genes in the *C. elegans* genome, 19 of which encode functional proteins (Ketting et.al, 2021). The microRNA pathway uses three AGO proteins: ALG-1, ALG-2 and ALG-5 (Ketting et. al, 2021). ALG-1 and ALG-2 are considered the major AGOs responsible for controlling the somatic microRNA pathway (Grishok et al., 2001) whereas the third member, ALG-5, couples specifically with miRNAs in the germline (Brown et al., 2017). ALG-1 and ALG-2 are highly similar in sequence, with 81% amino acid identity and structure (Vasquez-Rifo et al., 2012). However, microRNAs can preferentially associate with one over the other under specific cellular contexts (Brosnan et al., 2019). While this Argonaute loading preference has been attributed to differential expression of ALG-1 and ALG-2 (Brown et al., 2017), a recent study suggests an additional layer of AGO selection independent of cellular microRNA abundance (Brosnan et al., 2021). It has also been shown that ALG-1 and ALG-2 can associate with distinct proteins and assemble into different complexes (Tops et al., 2006).

Correspondingly, phenotypic studies suggest that the roles of ALG-1 and ALG-2 vary between different biological contexts. In the context of development, using RNAi to deplete both *alg-1* and *alg-2* results in embryonic lethality. Loss of function *alg-1* genetic mutant animals display more severe developmental delay compared to *alg-2* mutant animals, suggesting partial redundancy with *alg-1* playing a more important role during development

(Grishok et al., 2001; Vanquez-Rifo et al., 2012). In the context of aging, different from the synergistic effects seen in development, loss of ALG-1 or ALG-2 resulted in opposite lifespan-altering effects. Compared to wild-type, *alg-1* genetic mutants experienced reduced lifespan whereas *alg-2* genetic mutants displayed an extended lifespan. (Aalto et al., 2018). Of the thousands of misregulated genes found within the genetic mutants, many are characterized as genes associated with promoting or suppressing *C. elegans* longevity through the insulin/insulin-like growth factor signaling (IIS) pathway (Aalto et al., 2018; Murphy et al., 2003). Both genetic mutants act through the IIS pathway, as the extended lifespan of *alg-2* mutants is dependent on *daf-16,* a key transcription factor that promotes longevity (REF). Whereas, *alg-1* appears to be involved in additional aging-related pathways (Aalto et al., 2018).

Methods for Studying ALG-1 and ALG-2 Function in *C. elegans*

Since their identification, genetic mutants *alg-1(gk214)* and *alg-2 (ok304)* (Grishok et al., 2001) have been broadly used to study miRNA function in *C. elegans*. Developmental timing, brood size and lifespan assays have been conducted with the *alg-1* and *alg-2* mutants to characterize the role of the miRNA pathway under different biological contexts (Grishok et al., 2001; Vasquez-Rifo et al., 2012; Aalto et al., 2018). Phenotypes of *alg-1* and *alg-2* genetic mutants are often replicated using RNAi targeting *alg-1* and *alg-2* mRNA (Grishok et al., 2001; Aalto et al., 2018). These characterized phenotypes serve as important reference points, which direct studies to pinpoint specific microRNA and target genes involved in

distinct biological contexts. RNA-sequencing, qPCR, and Northern blots are common ways to look at mRNA changes upon loss of AGO function under desired biological contexts (Aalto et al., 2018; Pagliuso et al., 2021). Crosslinking immunoprecipitation and sequencing (CLIP-seq) is another valuable tool for studying AGO function, as it allows for direct detection of miRNA target mRNAs *in vivo*. This method has been applied in *C. elegans* to identify targets of ALG-1 (Broughton et al., 2016). Together, these methods and others have elucidated numerous contexts in which the miRNA pathway is critical for proper organismal function.

Chapter 2

Auxin Inducible Degron system offers conditional depletion of ALG-1 and ALG-2

Introduction

Given the central role of ALG-1 and ALG-2 in the microRNA pathway, knockdown or knockout of ALG-1 and ALG-2 together would allow researchers to block the somatic microRNA pathway. The genetic loss of function mutants, *alg-1(gk214)* and *alg-2(ok304)*, have provided valuable information to characterize the microRNA pathway's involvement in multiple biological contexts and identify the major microRNA targets. One interesting phenotypic observation from these genetic mutants is the aforementioned differential lifespan phenotypes arising from loss of *alg-1* or *alg-2*, hinting at their involvement in aging pathways (Aalto et al., 2018). Indeed, experimental data generated from the *alg-1* and *alg-2* genetic mutants have provided valuable information on the involvement of the miRNA pathway in aging on a molecular level (Aalto et al., 2018).

A major limitation towards using genetic mutants for studying the miRNA pathway in *C. elegans* is that loss of *alg-1* and *alg-2* together results in embryonic lethality (Vasquez et al., 2012). To study the function of the entire microRNA pathway during adulthood using the genetic mutants, other methods like RNAi must be used to deplete the second argonaute after development (Aalto et al., 2018). Additionally, the microRNA pathway is highly dynamic, with different microRNAs turning on at different time points and undergoing drastically

different expression trajectories. For example, the first discovered microRNA, let-7, which controls the transition between developmental stages of L4 to adult becomes detectable via northern blotting after worms have reached the third larval stage (L3) (Roush and Slack, 2008). Therefore, a more time resolved method to eliminate miRNA function would be beneficial to understand the role of the miRNA pathway and the function of specific miRNAs, such as let-7. As a result, loss of function (LOF) approaches suitable for removal of ALG-1 and ALG-2 need to provide rapid and reversible conditional depletion to better understand the function of these proteins and thus the involvement of microRNAs during important biological processes like aging.

Due to its relative ease of administration, another commonly used approach in *C. elegans* to reduce the expression of proteins of interest is RNAi (Conte et al., 2015). This LOF approach works on an RNA level, utilizing double-stranded RNA to direct the cleavage of mRNA targets of interest (Fire et al., 1998). However, knockdown via RNAi comes with certain drawbacks. RNAi often results in residual target mRNA expression. Further, its effectiveness is dependent on the natural half-life of target proteins (Housden et al., 2017). Additionally, off-target effects of RNAi, which cause unwanted non-target degradation might further complicate experimental results. Lastly, while there are recent advancements achieving reversible RNAi through photoresponsive siRNA (Matthew et al., 2020), established RNAi protocols in *C. elegans* do not offer efficient reversible degradation. As a result, while RNAi remains a powerful LOF tool in *C. elegans*, these drawbacks limit its utility in studying ALG-1 and ALG-2, given the dynamic nature of the microRNA pathway.

The auxin Inducible Degron (AID) is a novel degradation system that offers rapid and conditional depletion of a target protein. Originating from the auxin-dependent degradation pathway in plants, the AID system involves three basic components: degron-tagged protein target, transport inhibitor response 1 (TIR-1) protein expression in the target organism and the plant hormone auxin. Under the presence of auxin, the degron-tagged protein will be recognized by TIR1 as part of the E3 ubiquitin ligase SCF-TIR1 complex (Nishimura et al., 2009). This leads to polyubiquitylation on the degron and ultimately degradation of the target protein. As AID-mediated conditional degradation is rapid and reversible (Nishimura et al., 2009), its application to the miRNA pathway in *C. elegans* for conditional depletion of ALG-1 and ALG-2 seemed promising.

However, the first attempts at applying the AID system in *C. elegans* revealed major drawbacks. We observed basal degradation of degron-fused proteins without the presence of auxin (Schiksnis et al., 2020). More specifically, degron-tagged ALG-1, when co-expressed with TIR1, is depleted to approximately 30% of levels relative to wild-type (Schiksnis et al., 2020). Additionally, the AID system required a high-level of auxin (100-500uM) to achieve sufficient degradation (Yesbolatova et al, 2020). This is troubling, as exposing *C. elegans* to high levels of auxin (1mM and above) will result in increased lifespan (Loose and Ghazi, 2021). Given the significant involvement of ALG-1 and ALG-2 in aging and the sensitivity of the microRNA pathway, an improved AID system that addresses the two concerns was needed.

An improved AID system that utilizes a new TIR1 and auxin-analog, 5-Ph-IAA, termed Auxin Inducible Degron 2 (AID2) has been reported to overcome the two drawbacks, offering more robust degradation at lower auxin concentrations, along with no leaky degradation (Hills-Muckey et al., 2022; Yesbolatova et al, 2020). The goal of this thesis was to create improved tools for rapid and conditional degradation of ALG-1 and ALG-2 to further understand the activity and effects of the microRNA pathway, particularly in the context of aging. This project aimed to verify the improved AID2 system on an existing degron-tagged ALG-1 strain, create and validate a degron-tagged ALG-2 strain, and use these tools to replicate the lifespan effects seen previously in genetic mutants and corresponding RNAi treatments (Aalto et al., 2018).

Results

Generation of degron-tagged ALG-2 for use with the AID2 system

The AID2 system involves the degron-tagged protein target of interest, AID2 TIR1(F79G) (simplified as TIR1*) and auxin analog 5-pH-IAA (simplified as auxin). In addition to an available strain with degron::ALG-1 that carries TIR1*, fully silencing the microRNA pathway required the creation of degron tagged ALG-2. For the ease of visualization and detection, a GFP (mNeonGreen) and protein tag (3xflag) were in the design of the degron-tagged ALG-2. The insertions were placed at the 5'-end of *alg-2*, before the second exon of isoform a and the first exon of isoform b, where previous *alg-2* recombination showed successful integration (Aalto et al., 2018). After assembling the plasmid carrying the inserts and

homology sequences through Gibson assembly (Gibson et al., 2009), CRISPR/Cas9 genome editing was used to generate degron::mNeonGreen::3xflag::*alg-2* (PQ668 or degron::ALG-2) (Fig 1). Subsequently, degron::ALG-2 was crossed with degron::ALG-1; TIR1 (PQ667 or ALG-1^{AID}) to create degron::ALG-2; TIR1 (PQ671 or ALG-2^{AID}) and degron::ALG-1; degron::ALG-2; TIR1 (PQ670 or ALG-1^{AID}ALG-2^{AID}).

Degron-tagged ALG-1 and ALG-2 show no basal degradation using the AID2 system

To verify that the AID2 system does not cause leaky degradation of degron-fused protein in the presence of pan-somatic TIR1*, a Western blot targeting ALG-2 was performed to compare the protein levels of degron fused ALG-2 in animals expressing TIR1* (ALG-2^{AID}) and without TIR1* expression (degron::ALG-2) (Fig 2a). Western blot results demonstrate that ALG-2 protein level does not change in the presence of the TIR1*, supporting the conclusion that the AID2 system does not cause leaky degradation of degron fused ALG-2 (Fig 2a).

To further verify a lack of basal degradation of the dual degron-tagged ALG-1 and ALG-2 strain (ALG-1^{AID}ALG-2^{AID}) when TIR1* is expressed, a brood size assay was performed. Given that *alg-1(gk214)* exhibits a significantly reduced brood size, basal degradation of ALG-1 in the degron::ALG-1 strain would be expected to lead to a reduction in brood size. The assay was conducted using wild-type, as well as *alg-1(gk214)* and *alg-2(ok304)* genetic mutants as controls. The brood size results suggest no auxin-independent degradation of

degron::ALG-1 when paired with degron::ALG-2, as the brood size closely matches that of wild-type (Fig. 2b). In a separate experiment, ALG-1^{AID} also exhibits a wild-type brood size when expressing TIR1*, in contrast to the reduced brood size produced by *alg-1(gk214)* (Fig. 2c). It is worth noting that *alg-2(ok304)* has been characterized by other labs to also reduce brood size, though not as severe as *alg-1(gk214).* This reduction in brood size however, was not seen in our experiments (Fig 2b). Overall, the brood size result suggests no leaky degradation of ALG-1 under TIR1* with the ALG-2^{AID} and ALG-1^{AID}ALG-2^{AID} strains all showing wild-type levels of offspring, while *alg-1(gk214)* shows the expected significantly reduced brood size (Fig 2b and 2c).

The AID2 system allows for rapid degradation of ALG-1 and ALG-2 with low auxin concentrations

Considering reported lifespan-extending effects of auxin in *C. elegans* at high concentrations (1mM and above) (Loose and Ghazi, 2021), it was important to verify that the AID2 system would deplete degron::ALG-1/2 at low auxin concentrations (1uM-30uM). To verify sufficient degradation of degron::ALG-1 and degron::ALG-2, a western blot was used to compare the ALG-1 and ALG-2 levels at matched time points with or without auxin added to growth media, for the three strains of ALG-1^{AID}, ALG-2^{AID} and ALG-1^{AID}ALG-2^{AID}. Exposure of synchronized larval stage 4 (L4) worms to 30uM auxin, led to full depletion of ALG-1 after 4.5 hours of auxin treatment compared to no auxin control (Fig 3a). While both ALG-1 and ALG-2 are tagged with FLAG and thus should be detectable with the same anti-FLAG antibody, we were unable to specifically detect ALG-2 under exposure levels adjusted for

ALG-1, as ALG-1 is much more highly expressed during L4 (Aalto et al., 2018). At higher exposure levels, loss ALG-2 signal can be visualized within ALG2^{AID} using this antibody which suggests complete degradation of ALG-2 (Fig 3b)

To specifically verify and fully characterize auxin-induced degradation of degron::ALG-2, another Western blot comparing degron::ALG-2 protein levels under differing auxin concentrations of 1uM, 5uM, 10uM and 30uM and differing auxin treatment time points ranging from 1 hour to 6 hours was conducted on degron::ALG-2 (Fig. 3c and 3d). For all the tested conditions, no remaining ALG-2 was seen upon auxin treatment. Overall, complete degradation of ALG-2 can be achieved with minimal auxin concentration of 1uM and minimal treatment time of 1 hour (Fig 3d). As another way of verifying the effectiveness of degradation, fluorescent microscopy was used to compare the levels of ALG-2^{AID} after 3hrs of 10uM auxin treatment against no auxin control (Fig 3e). Together, these results confirm that the AID2 system is robust in depletion of ALG-1 and ALG-2, eliminates basal degradation at examined time points, and allows for use of much lower auxin concentrations.

Depletion of ALG-1 and ALG-2 with the AID2 system replicates lifespan phenotypes of genetic mutants

Given the potential utility of degron::ALG-1/2 strains in studying the roles of ALG-1 and ALG-2 during aging, lifespan assays were conducted to see if the lifespan altering effects observed in the genetic mutant and RNAi treatments are recapitulated using this improved tool. ALG-1^{AID} and ALG-2^{AID} lifespans were compared on auxin to non-auxin controls. As with

the time point used for feeding RNAi (Aalto et al., 2018), a cohort of animals was moved onto auxin plates at 48 hours (L4), while the control cohort was moved onto plates not supplemented with auxin (Fig. 4a). The auxin concentration used was 10uM, 100-fold lower than the documented auxin concentration where lifespan extending effects occur (Loose and Ghazi, 2021). While only one replicate of the lifespan assay has been done so far, ALG-1^{AID} and ALG-2^{AID} strains showed lifespan reducing or extending effects respectively under auxin conditions ($p < 0.05$) (Fig 4b and Fig 4c), reflecting the patterns seen in the genetic mutants and RNAi (Aalto et al., 2018). Additionally, wild-type *C. elegans* (N2) showed no significant difference in lifespan between auxin and control conditions, suggesting that the lifespan effects are not due to auxin and are the result of loss of ALG-1 or ALG-2. This result, if repeated, also confirms that the AID2 system is more useful in the context of aging, as lower concentrations of auxin do not affect lifespan, contrary to concentrations required to deplete proteins in the original system.

Discussion

Based on western and imaging analysis, the AID2 system offers rapid degradation ALG-1 and ALG-2 with no basal degradation. Thus, the new ALG-1^{AID} and ALG-2^{AID} strains promise great utility in aging studies. To begin with, lifespan results and molecular aging data generated from the *alg-1* and *alg-2* genetic mutants might be subject to the damages accumulated during development due to a chronic defect in the microRNA pathway. Results from RNAi against *alg-1* or *alg-2*, risk off-target effects along with insufficient depletion of the argonaute targets. By rapid degradation of ALG-1 and ALG-2 after development, the AID2

system can more accurately reveal the immediate effects of knocking down the entire microRNA pathway. Additionally, ALG-1^{AID} and ALG-2^{AID} can be used to shut down ALG-1 and ALG-2 within specific timeframes in aging *C. elegans*. This could provide valuable information to decode the underlying mechanisms behind the differential lifespan altering effects of *alg-1* and *alg-2*. Lastly, tissue specific ALG-1 and ALG-2 degradation can be achieved using TIR1 with tissue-specific promoters (Ashley et al., 2021).

Whether ALG-1^{AID} and ALG-2^{AID} produce the changes in target mRNA and microRNA levels previously observed in the genetic mutant strains in adult *C. elegans* remains to be tested (Aalto et al., 2018). Another strategy to test how well ALG-1^{AID} and ALG-2^{AID} can phenocopy the genetic mutants is to test for embryonic lethality in backgrounds where the activity of both Argonautes is lost. This should be examined in the ALG-1^{AID}ALG-2^{AID} strain as well as in strains with ALG-1^{AID} crossed to *alg-2(ok304)* and ALG-2^{AID} crossed to *alg-1(gk214)*. A functional AID2 system should knockdown the degron-tagged Argonautes under the presence of auxin and result in embryonic lethality when both ALG-1 and ALG-2 are depleted.

One major concern with the depleting ALG-1 via AID2 is the inability to reproduce alg-1 phenotypes in developing worms. Based on the work from another lab member, auxin treatment against ALG-1^{AID}ALG-2^{AID}, even after prolonged exposure (7hrs), showed no changes in the mRNA levels of known ALG-1 targets such as ins-33, daf-12 and lin41 relative to wild-type (N2) through qPCR at L4 timepoint (29hrs). In comparison, these genes

are highly upregulated in *alg-1(gk214)* at this timepoint. Similarly, TaqMan assay against let-7, which is significantly downregulated in *alg-1*, showed no change in expression under the same experimental conditions. There are some hypotheses that could explain this discrepancy between ALG-1 protein degradation and no change in the microRNA pathway. One initial concern was that prolonged auxin exposure might result in *C. elegans* resisting auxin. However, since ALG-2 levels showed no resurgence between 1hr-6hrs auxin treatment, it does not appear that worms buildup auxin resistance overtime. To fully rule out this possibility, ALG-1 degradation by ALG-1^{AID} also must be verified at multiple timepoints after auxin treatment. Since the degron and Flag tag are both located at the 5'end of *alg-1*, another possibility was that ALG-1 protein might undergo a cleavage process at the N terminus. However, no fragment was observed with FLAG tag. It might also be possible that the protein structure/ modifications of ALG-1 stopped the degradation midway and the remaining portion was still able to function in the RISC complex. One way to test this hypothesis is to capture ALG-1 with antibodies that recognize peptide sequences further away from the N terminus. One challenge is that protein tags near the C terminus of ALG-1 will result in a non-functional product. As a result, antibodies that target ALG-1 in this region are needed. Human AGO2 antibodies were attempted, as both Argonautes share levels of similarity, yet we were unable to detect *C. elegans* ALG-1. Lastly, the degron sequences in ALG-1^{AID} and ALG-2^{AID} follow the original AID system, whereas the AID2 system verified in *C. elegans* uses a shorter mAID degron (Negishi et al., 2022). Despite these caveats, the ALG-1^{AID} and ALG-2^{AID} strains show great potential in studying the effects of the microRNA pathway especially in the context of aging.

Chapter 3

Investigation of the two let-7 binding sites in the *alg-1* 5'UTR

Introduction

The canonical microRNA pathway involves microRNA base-paring with complementary binding sites found within the 3'UTR of target transcripts for subsequent translational inhibition and/or mRNA degradation (Bartel, 2009). However, microRNA-target pairing algorithms revealed abundant amounts of 5'UTR microRNA binding sites within the mouse, drosophila and human genomes (Zhou et al., 2009). Some of the 5'UTR microRNA binding sites are functional and have a variety of effects ranging from the canonical mRNA degradation to promoting translation in different organisms (Lytle et al., 2007; Ørom et al., 2008; Schult et al., 2018). This project documents the identification of two let-7 binding sites within the 5'UTR of *alg-1* isoform a and my attempts to test if they serve any biological function.

Results

2 let-7 binding sites are found within 5'UTR of *alg-1* isoform a

The binding of let-7 in the *alg-1* 5'UTR was first revealed by FeatureCounts analysis of ALG-1 CLIP-seq results. Besides a strong peak of ALG-1 CLIP-seq reads located in the *alg-1* 5'UTR, chimeric reads consisting of let-7 ligated to *alg-1* 5'UTR sequence were also

detected (Liao et al., 2014; Broughton et al., 2016) (Fig 5a). To search for potential let-7 binding sites, RNA hybrid was used to align mature let-7 sequence with the 5'UTR of *alg-1* isoform a (F48F7.1a.2). Two sites complementary to the seed sequence of let-7, where let-7 would bind with high affinity, were observed (Fig 5b).

Removal of the let-7 binding sites within the *alg-1* 5'UTR does not affect ALG-1 expression

To study the role of let-7 binding to the *alg-1* 5'UTR, two new strains that lack the let-7 complementarity sites were created: Δalg15UTR-let7^{A}(PQ657) and Δalg15UTR-let7^{B} (PQ658). These two strains each have both of the let-7 complementary sites changed into sequences without predictable let-7 binding (Fig 6a). For easier quantification, the mutations were introduced within the GFP- and flag-tagged *alg-1* strain (PQ530), and this parent strain served as a control in future experiments.

qPCR was used to compare the *alg-1* mRNA levels between the mutants and control at L4, where ALG-1 is highly expressed (Aalto et al., 2018) (Fig 6b). Additionally, western blot was used to compare ALG-1 protein levels between the mutants and control (Fig 6c). Given qPCR and western results showing no detectable change in *alg-1* mRNA and ALG-1 protein levels between the two mutant and control (Fig 6b and 6c), the two let-7 binding sites do not seem to control ALG-1 expression at this time point.

Discussion

Overall, the two let-7 binding sites found within the 5'UTR of *alg-1* mRNA appear to be nonfunctional under normal conditions. Still, the appearance of microRNA target sites within the 5'UTR of *alg-1* and the functionality of microRNA complementary binding sites within the 5'UTR in general remains to be explored. There remains the possibility that these sites mediate regulation of *alg-1* expression at another stage or as part of a defense/ stress response mechanism. Interesting, previous work in human cell culture has shown that introducing 5'UTR let-7 binding sites will result in target degradation (Lytle et al., 2007). Overall, the idea of let-7 regulating ALG-1 as a negative feedback loop, perhaps in particular conditions such as let-7 overexpression at undesired timepoints, remains an interesting possibility to explore.

Figures

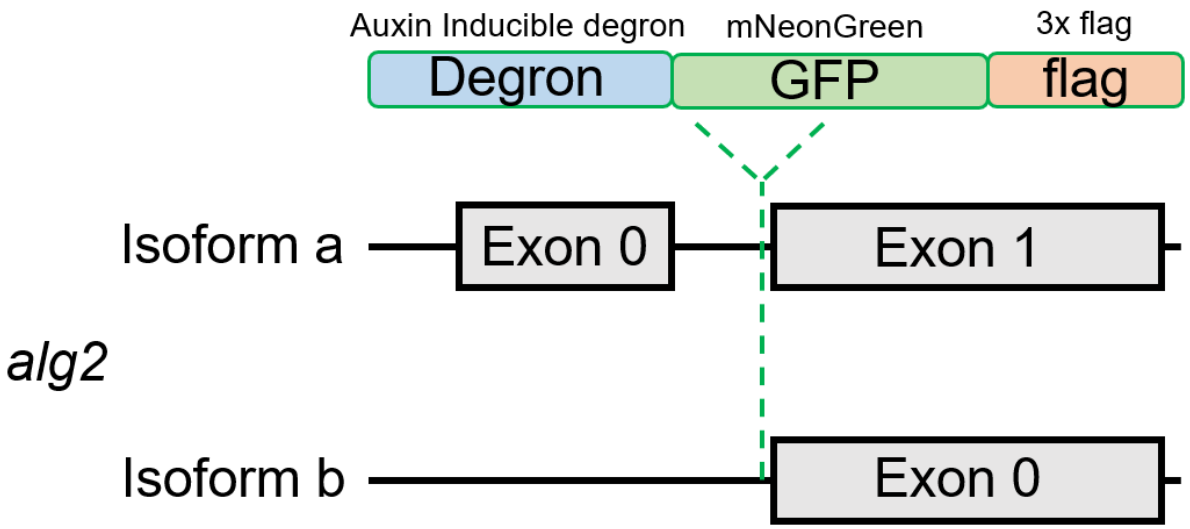

Figure 1: Illustration of AID::mNeonGreen:: 3xflag:: *alg-2* (degron::ALG-2 or PQ668). The components and location of the degron insertion complex is indicated for the two *alg-2* isoforms.

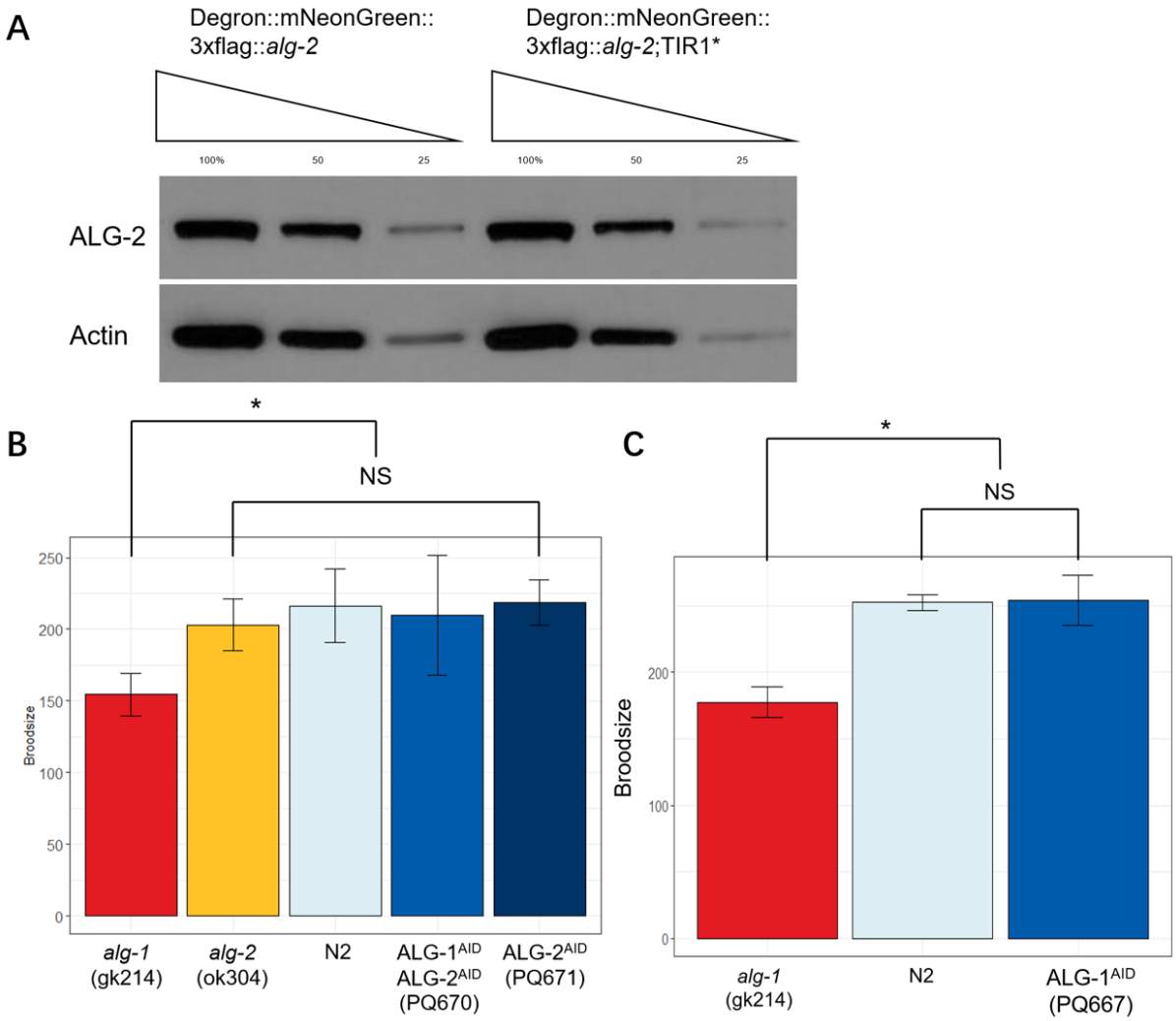

Figure 2: No basal degradation of degron-tagged ALG-1 or ALG-2. (A) Westen blot of ALG-2 protein levels in Degron::mNeonGreen::3xFLAG:: alg-2 (degron::alg2) and Degron::mNeonGreen::3xFLAG::ALG-2;TIR1*(ALG-2^{AID}). Actin serves as a loading control. (B and C) Brood size assay of *alg-1(gk214)*, *alg-2(ok304)*, N2, ALG-1AID+ALG-2AID and ALG-2AID and Brood size assay of *alg-1(gk214)*, N2 and ALG-1^{AID}. Each brood size assay include 3 Replicates.* p< 0.05 (log-rank) between *alg-1(gk214)* and all the other conditions in a two tailed t-test.

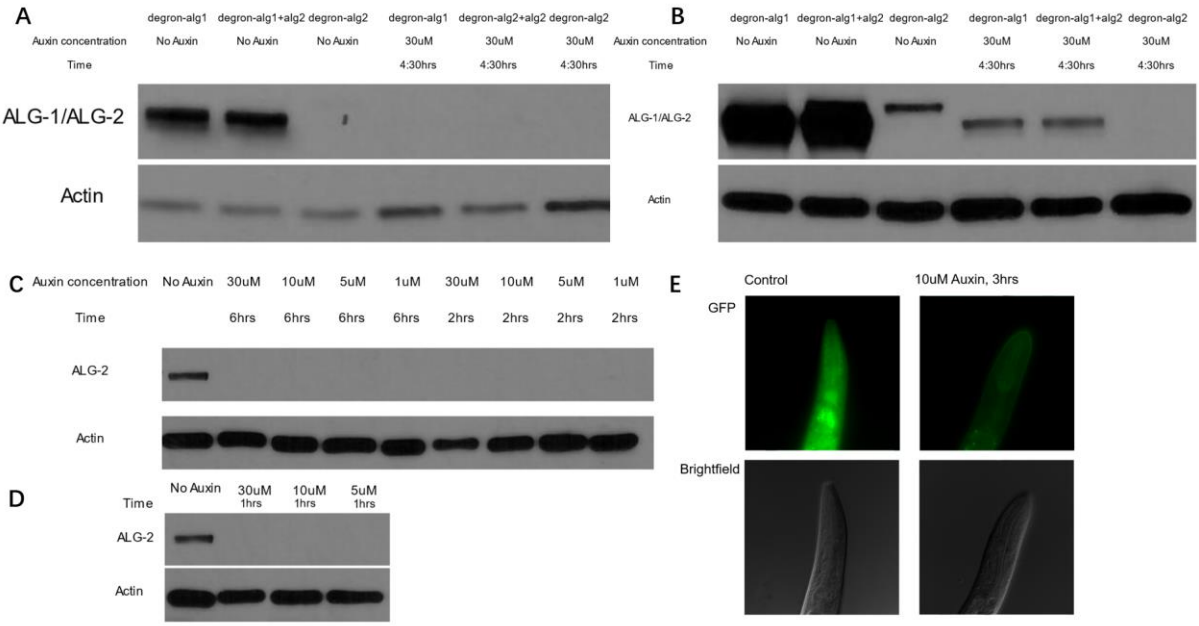

Figure 3: Degradation of ALG-1 and ALG-2 under various auxin treatments. (A and B) Western blot of ALG-1 protein levels in ALG-1^{AID}, ALG-1^{AID}ALG-2^{AID} and ALG-2^{AID} with or without 30uM auxin treatment for 4.5hrs, the exposure levels are adjusted for ALG-1 and ALG-2 respectively in A and B. Actin levels serve as a loading control. (C and D) Western blot of ALG-2 protein levels in Degron::mNeonGreen::3xflag::alg-2;TIR1* (ALG-2^{AID} or PQ671) under various auxin treatments for 6hrs, 2hrs and 1hrs. Actin levels serve as a loading control. （E） micrograph of Degron::mNeonGreen::3xFLAG:: ALG-2;TIR1* (ALG-2^{AID} or PQ671) under auxin or control conditions.

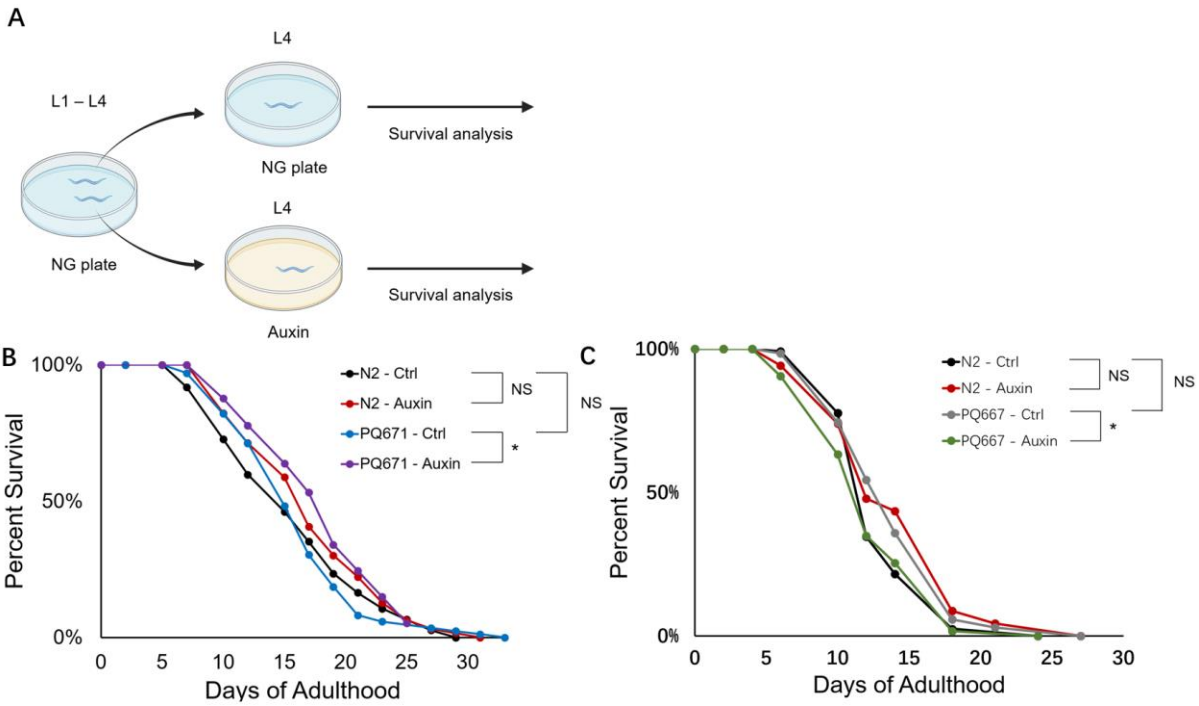

Figure 4: Depletion of ALG-1 and ALG-2 with the AID2 system reduces and extends lifespan. (A) Schematic of the lifespan protocol. Worms were raised at NG plate until L4, and then moved to either NG plates (control) or Auxin plates. Worms were moved every other day onto new plates until egg laying stopped. (B) Survival curves showing increased lifespan of Degron::mNeonGreen::3xFLAG::alg2; TIR1*(ALG-2^{AID} or PQ671), on auxin compared with off auxin. *P<0.05 (log-rank). (C) Survival curves showing reduced lifespan in Degron::4xFLAG::alg1; TIR1* (ALG-1^{AID} or PQ667) on auxin compared with off auxin. *P<0.05 (log-rank).

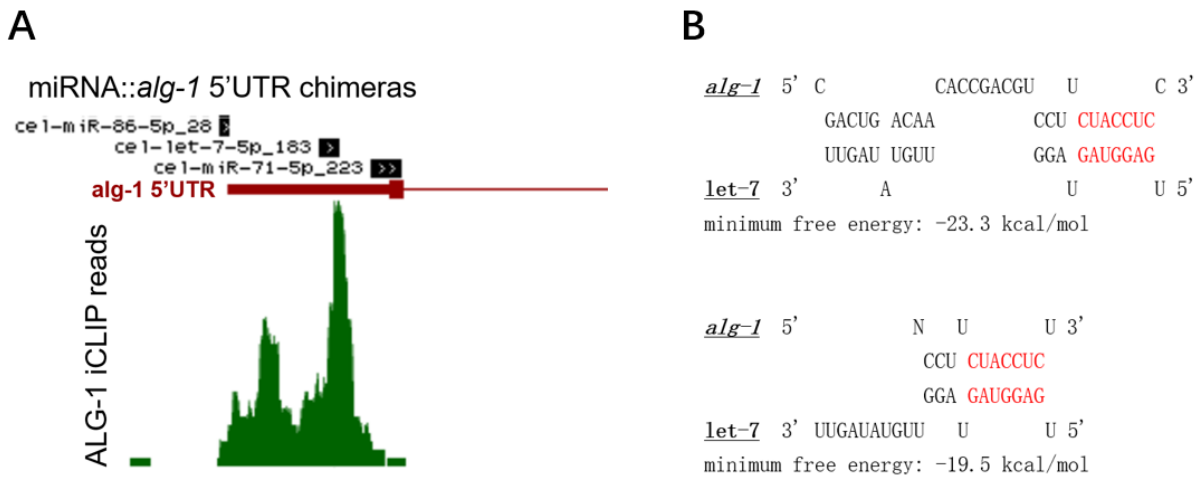

Figure 5: Let-7 binds to the 5'UTR of *alg-1* isoform a. (A) Featurecounts alignment of iCLIP result showing strong binding of ALG-1 within the *alg-1* isoform a 5'UTR. Green peaks represent binding of ALG-1. (B) RNA hybrid predicts two let-7 binding sites within the 5'UTR of *alg-1* isoform a.

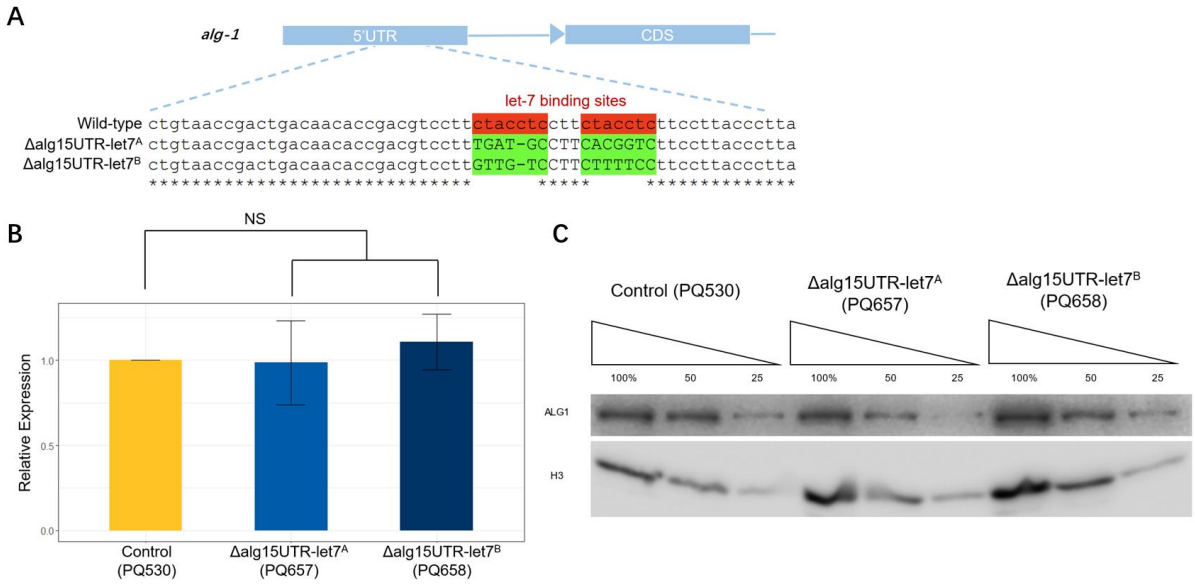

Figure 6: Disrupted let-7 binding sites does not change *alg-1* expression. (A) Sequence alignment within *alg-1* isoform a 5'UTR showing the two let-7 complementary binding sites (red) in wild-type and the disrupted binding sequence within two mutants Δalg15UTR-let7A (PQ657) and Δalg15UTR-let7A (PQ658) (green). (B) qPCR shows no change in *alg-1* mRNA level in L4 worms between 3xFLAG::gfp::alg-1 (PQ530) and mutants with disrupted binding sites: Δalg15UTR-let7A (PQ657) and Δalg15UTR-let7A (PQ658) (C) Westen blot shows no change in ALG-1 protein levels in L4 worms between 3xFLAG::gfp::alg-1 (PQ530) and mutants with disrupted binding sites: Δalg15UTR-let7A (PQ657) and Δalg15UTR-let7A (PQ658). Histone 3 (H3) levels serve as loading control.

Materials and Methods

Pouring and handling of auxin plates

The appropriate amount of 5-ph-IAA was added as the last step before pouring following standard NGM plate protocols. All auxin plates are kept in a dark environment except for collection/ analysis.

C. elegans lifespan analysis

Lifespan analyses were conducted at 20^{o}C in the absence of FUdR (Dillin et al., 2002). Embryos are plated on NGM plates containing OP50 and moved upon their respective auxin-containing plates or no-auxin control plates. Worms were moved onto fresh plates every other day until reproduction stopped, survival measured every 2-3 days. Worms censored include: ruptured vulvas, bagged, trapped or contaminated. JMP IN 8.0 software was used for statistical analysis and P-values were calculated using the log-rank (Mantel-Cox) method.

Brood size analysis

Brood size analyses were conducted at 20^{o}C. Synchronized L1 worms were plated on NGM plates containing OP50 and >5 worms representing each treatment were moved onto individual plates at L4 (48hrs). After D1 (72hrs), worms are moved onto fresh plates every 1-2 days and with embryos and larva number recorded until egg-laying stopped. Animals censored include: ruptured vulvas, bagged, trapped or contaminated.

Western blotting

Western blot was performed as previously described (Wynsberghe et al., 2011) with mouse monoclonal antibodies against FLAG (Sigma), actin or Histone 3.

Fluorescent Imaging

PQ671 animals were cultured at 20^{o}C and grown until 34hr before moving onto auxin (10uM)/ no auxin control plates for 3hrs. For imaging, worms were anesthetized with 1mg/ul Levamisole and imaged at 40X magnification. Imaging was performed with Zeiss Axio Imager.A1.

qRT-PCR

Quantitative RT-PCR analyses of mRNA (SYBR Green) levels were performed according to manufacturer’s instructions with QuantStudio 3 Real-Time PCR Systems (Applied

Biosystems). mRNA Levels were normalized to Y45F10D.4.

Let-7 binding site identification and designing of disrupted binding site

FeatureCounts was used to assign reproducible ALG-1 miRNA-target reads (Broughton et al., 2016) to annotated 5'UTR features in the *C. elegans* genome (Liao et al., 2014). The mature *C. elegans* let-7 sequence was aligned to the *alg-1* 5'UTR sequence using RNAhybrid (Rehmsmeier et al., 2004). Repair templates that replace the two predicted let-7 target sites with sequences not predicted to bind other *C. elegans* miRNAs were designed using ImiRP (Ryan et al., 2016)

Nematode culture and strains

Strains were maintained at 20ºC. Worm strains: Bristol N2 (WT), VC446 (*alg-1(gk214)*), WM53 (*alg-2(ok304)*), PQ530 (*alg-1*(ap423 [3xflag::gfp::*alg-1*])). PQ657 (*alg-1*(ap440xap423[3xflag::gfp::*alg-1*])), PQ658 (*alg-1*(ap441xap423[3xflag::gfp::*alg-1*])), PQ668 (*alg-2*(ap444[aid::mNeonGreen::3xflag::*alg-2* crispr])). The following *C. elegans* strains were generated through crosses: PQ667 (cshIs140 [rps-28p::TIR1(F79G)::T2A::mCherry::his-11 + Cbr-unc-119(+)] II; *alg-1*(xk20)[aid::4xflag::*alg-1*]), PQ670 (cshIs140[rps-28p::TIR1(F79G)::T2A::mCherry::his-11 + Cbr-unc-119(+)] II; *alg-1*(xk20)[aid::4xflag::*alg-1*; II *alg-2*(ap444)[aid::mNeonGreen::3xflag::*alg-2*], PQ671 (*alg-2*(ap444)[aid::mNeonGreen::3xflag::*alg-2*] II; cshIs140[rps-28p::TIR1(F79G)::T2A::mCherry::his-11 + Cbr-unc-119(+)] II)

Genome editing to produce tagged and modified endogenous genes

CRISPR/Cas9 Genome editing methods were used to generated novel worm strains (Tzur et al., 2013). To make the PQ657 strain (*alg-1*(ap440xap423[3xflag::gfp::*alg-1*])), young adult PQ530 worms (*alg-1*(ap423 [3xflag::gfp::*alg-1*])) were injected with repair template ap440, sgRNA, and Cas9 following the ssODN CRISPR protocol for generating point mutations (Paix et al., 2017). Strains were then backcrossed to PQ530 animals four times to produce PQ657. ap440: 5'-
CGAATCTGTAACCGACTGACAACACCGACGTCCTTGTTGTCCTTCTTTTCCTTCCTTACC
CTTATTATTGCTTTAAAAGGATACAA-3'
sgRNA: 5'-CUUCCUUACCCUUAUUAUUG-3'

To make the PQ658 strain ((*alg-1*(ap441xap423[3xflag::gfp::*alg-1*]))), young adult PQ530 worms (*alg-1*(ap423 [3xflag::gfp::*alg-1*])) were injected with repair template ap441, sgRNA, and Cas9 following the ssODN CRISPR protocol for generating point mutations (Paix et al., 2017). Strains were then backcrossed to PQ530 animals four times to produce PQ658.
ap441: 5'-
CGAATCTGTAACCGACTGACAACACCGACGTCCTTTGATGCCTTCACGGTCTTCCTTAC
CCTTATTATTGCTTTAAAAGGATACAA-3'
sgRNA: 5'-CUUCCUUACCCUUAUUAUUG-3'

To make the strain PQ668 (*alg-2*(ap444[aid::mNeonGreen::3xflag::*alg-2* crispr])), young adult N2 animals were injected with the following plasmids: 50ng/ul of homologous repair template (aid::mNeonGreen::3xflag with ALG-2 homology arms, constructed following Gibson assembly protocol using PDD268),50ng/ul pJB53 (Cas9 plasmid with ALG-2 specific sgRNA, a modification of pJW1219 (a gift from Jordan Ward, Addgene #61250), 10ng/ul pGH8 (pRAB-3::mCherry::unc-54utr, a gift from Erik Jorgensen, Addgene plasmid #19359) 5ng/μL pCFJ104 (Pmyo-3::mCherry::unc-54; a gift from Erik Jorgensen; Addgene plasmid #19328), 2.5ng/ul pCFJ90 (Pmyo-2::mCherry::unc-54utr; a gift from Erik Jorgensen; Addgene plasmid #19327). Isolation of recombinants was performed as described in Dickinson, et al. 2015 (Dickinson et al. 2015). Strains were then backcrossed 3x to N2 to generate PQ668.

References

Aalto, A. P., Nicastro, I. A., Broughton, J. P., Chipman, L. B., Schreiner, W. P., Chen, J. S., & Pasquinelli, A. E. (2018). Opposing roles of microRNA Argonautes during Caenorhabditis elegans aging. *PLOS Genetics*, *14*(6), e1007379. https://doi.org/10.1371/journal.pgen.1007379

Alvarez-Saavedra, E., & Horvitz, H. R. (2010). Many Families of C. elegans MicroRNAs Are Not Essential for Development or Viability. *Current Biology*, *20*(4), 367–373. https://doi.org/10.1016/j.cub.2009.12.051

Bartel, D. P. (2009). MicroRNAs: Target Recognition and Regulatory Functions. *Cell*, *136*(2), 215–233. https://doi.org/10.1016/j.cell.2009.01.002

Bartel, D. P. (2018). Metazoan MicroRNAs. *Cell*, *173*(1), 20–51. https://doi.org/10.1016/j.cell.2018.03.006

Brosnan, C. A., Palmer, A. J., & Zuryn, S. (2021). Cell-type-specific profiling of loaded miRNAs from Caenorhabditis elegans reveals spatial and temporal flexibility in Argonaute loading. *Nature Communications*, *12*(1), 2194. https://doi.org/10.1038/s41467-021-22503-7

Broughton, J. P., Lovci, M. T., Huang, J. L., Yeo, G. W., & Pasquinelli, A. E. (2016). Pairing beyond the Seed Supports MicroRNA Targeting Specificity. *Molecular Cell*, *64*(2), 320–333. https://doi.org/10.1016/j.molcel.2016.09.004

Brown, K. C., Svendsen, J. M., Tucci, R. M., Montgomery, B. E., & Montgomery, T. A. (2017). ALG-5 is a miRNA-associated Argonaute required for proper developmental timing in the Caenorhabditis elegans germline. *Nucleic Acids Research*, *45*(15), 9093–9107. https://doi.org/10.1093/nar/gkx536

Conte Jr., D., MacNeil, L. T., Walhout, A. J. M., & Mello, C. C. (2015). RNA Interference in Caenorhabditis elegans. *Current Protocols in Molecular Biology*, *109*(1), 26.3.1-26.3.30. https://doi.org/10.1002/0471142727.mb2603s109

Denli, A. M., Tops, B. B. J., Plasterk, R. H. A., Ketting, R. F., & Hannon, G. J. (2004). Processing of primary microRNAs by the Microprocessor complex. *Nature*, *432*(7014), 231–235. https://doi.org/10.1038/nature03049

Fire, A., Xu, S., Montgomery, M. K., Kostas, S. A., Driver, S. E., & Mello, C. C. (1998). Potent and specific genetic interference by double-stranded RNA in Caenorhabditis elegans. *Nature*, *391*(6669), 806–811. https://doi.org/10.1038/35888

Gibson, D. G., Young, L., Chuang, R.-Y., Venter, J. C., Hutchison, C. A., & Smith, H. O. (2009). Enzymatic assembly of DNA molecules up to several hundred kilobases. *Nature Methods*, *6*(5), 343–345. https://doi.org/10.1038/nmeth.1318

Grishok, A., Pasquinelli, A. E., Conte, D., Li, N., Parrish, S., Ha, I., Baillie, D. L., Fire, A., Ruvkun, G., & Mello, C. C. (2001). Genes and Mechanisms Related to RNA Interference Regulate Expression of the Small Temporal RNAs that Control C. elegans Developmental Timing. *Cell*, *106*(1), 23–34. https://doi.org/10.1016/S0092-8674(01)00431-7

Hills-Muckey, K., Martinez, M. A. Q., Stec, N., Hebbar, S., Saldanha, J., Medwig-Kinney, T. N., Moore, F. E. Q., Ivanova, M., Morao, A., Ward, J. D., Moss, E. G., Ercan, S., Zinovyeva, A. Y., Matus, D. Q., & Hammell, C. M. (2022). An engineered, orthogonal auxin analog/AtTIR1(F79G) pairing improves both specificity and efficacy of the auxin degradation system in Caenorhabditis elegans. *Genetics*, *220*(2), iyab174. https://doi.org/10.1093/genetics/iyab174

Housden, B. E., Muhar, M., Gemberling, M., Gersbach, C. A., Stainier, D. Y. R., Seydoux, G., Mohr, S. E., Zuber, J., & Perrimon, N. (2017). Loss-of-function genetic tools for animal models: Cross-species and cross-platform differences. *Nature Reviews Genetics*, *18*(1), 24–40. https://doi.org/10.1038/nrg.2016.118

Lee, R. C., Feinbaum, R. L., & Ambros, V. (1993). The C. elegans heterochronic gene lin-4 encodes small RNAs with antisense complementarity to lin-14. *Cell*, *75*(5), 843–854. https://doi.org/10.1016/0092-8674(93)90529-Y

Lewis, B. P., Shih, I., Jones-Rhoades, M. W., Bartel, D. P., & Burge, C. B. (2003). Prediction of Mammalian MicroRNA Targets. *Cell*, *115*(7), 787–798. https://doi.org/10.1016/S0092-8674(03)01018-3

L. Hammill, M., Islam, G., & Desaulniers, J.-P. (2020). Reversible control of RNA interference by siRNAzos. *Organic & Biomolecular Chemistry*, *18*(1), 41–46. https://doi.org/10.1039/C9OB02509J

Loose, J. A., & Ghazi, A. (2021). Auxin treatment increases lifespan in Caenorhabditis elegans. *Biology Open*, *10*(5), bio058703. https://doi.org/10.1242/bio.058703

Lytle, J. R., Yario, T. A., & Steitz, J. A. (2007). Target mRNAs are repressed as efficiently by microRNA-binding sites in the 5′ UTR as in the 3′ UTR. *Proceedings of the National Academy of Sciences*, *104*(23), 9667–9672. https://doi.org/10.1073/pnas.0703820104

Murphy, C. T., McCarroll, S. A., Bargmann, C. I., Fraser, A., Kamath, R. S., Ahringer, J., Li,

H., & Kenyon, C. (2003). Genes that act downstream of DAF-16 to influence the lifespan of Caenorhabditis elegans. *Nature*, *424*(6946), 277–283. https://doi.org/10.1038/nature01789

Negishi, T., Kitagawa, S., Horii, N., Tanaka, Y., Haruta, N., Sugimoto, A., Sawa, H., Hayashi, K., Harata, M., & Kanemaki, M. T. (2022). The auxin-inducible degron 2 (AID2) system enables controlled protein knockdown during embryogenesis and development in Caenorhabditis elegans. *Genetics*, *220*(2), iyab218. https://doi.org/10.1093/genetics/iyab218

Nishimura, K., Fukagawa, T., Takisawa, H., Kakimoto, T., & Kanemaki, M. (2009). An auxin-based degron system for the rapid depletion of proteins in nonplant cells. *Nature Methods*, *6*(12), 917–922. https://doi.org/10.1038/nmeth.1401

Ørom, U. A., Nielsen, F. C., & Lund, A. H. (2008). MicroRNA-10a Binds the 5′UTR of Ribosomal Protein mRNAs and Enhances Their Translation. *Molecular Cell*, *30*(4), 460–471. https://doi.org/10.1016/j.molcel.2008.05.001

Pagliuso, D. C., Bodas, D. M., & Pasquinelli, A. E. (2021). Recovery from heat shock requires the microRNA pathway in Caenorhabditis elegans. *PLOS Genetics*, *17*(8), e1009734. https://doi.org/10.1371/journal.pgen.1009734

Schiksnis, E. C., Nicholson, A. L., Modena, M. S., Pule, M. N., Arribere, J. A., & Pasquinelli, A. E. (n.d.). Auxin-independent depletion of degron-tagged proteins by TIR1. *MicroPublication Biology*, *2020*, 10.17912/micropub.biology.000213. https://doi.org/10.17912/micropub.biology.000213

Schult, P., Roth, H., Adams, R. L., Mas, C., Imbert, L., Orlik, C., Ruggieri, A., Pyle, A. M., & Lohmann, V. (2018). MicroRNA-122 amplifies hepatitis C virus translation by shaping the structure of the internal ribosomal entry site. *Nature Communications*, *9*(1), 2613. https://doi.org/10.1038/s41467-018-05053-3

Tops, B. B. J., Plasterk, R. H. A., & Ketting, R. F. (2006). The Caenorhabditis elegans Argonautes ALG-1 and ALG-2: Almost Identical yet Different. *Cold Spring Harbor Symposia on Quantitative Biology*, *71*, 189–194. https://doi.org/10.1101/sqb.2006.71.035

Vasquez-Rifo, A., Jannot, G., Armisen, J., Labouesse, M., Bukhari, S. I. A., Rondeau, E. L., Miska, E. A., & Simard, M. J. (2012). Developmental Characterization of the MicroRNA-Specific C. elegans Argonautes alg-1 and alg-2. *PLOS ONE*, *7*(3), e33750. https://doi.org/10.1371/journal.pone.0033750

Yesbolatova, A., Saito, Y., Kitamoto, N., Makino-Itou, H., Ajima, R., Nakano, R., Nakaoka, H., Fukui, K., Gamo, K., Tominari, Y., Takeuchi, H., Saga, Y., Hayashi, K., & Kanemaki,

M. T. (2020). The auxin-inducible degron 2 technology provides sharp degradation control in yeast, mammalian cells, and mice. *Nature Communications*, *11*(1), 5701. https://doi.org/10.1038/s41467-020-19532-z

Zhou, X., Duan, X., Qian, J., & Li, F. (2009). Abundant conserved microRNA target sites in the 5′-untranslated region and coding sequence. *Genetica*, *137*(2), 159–164. https://doi.org/10.1007/s10709-009-9378-7